Available online at www.sciencedirect.com

ScienceDirect

Nuclear Physics B Proceedings Supplement 00 (2015) 1–9

Nuclear Physics B Proceedings Supplement

Towards the equation of state of quark-gluon matter from lattice QCD with Wilson twisted mass fermions

F. Burger and M. Müller-Preussker

Humboldt-Universität zu Berlin, Institut für Physik, Newtonstr. 15, 12489 Berlin

Abstract

This contribution gives an overview of a long-term study of quark-gluon matter under extreme conditions employing Euclidean lattice discretized Quantum Chromodynamics (QCD) with Wilson twisted mass fermions and improved gauge actions. The analysis relies on methods and results of the European Twisted Mass Collaboration at zero temperature. We will start for two mass-degenerate light flavour degrees of freedom with a thorough investigation of the three-dimensional phase diagram of the bare coupling and the two mass-related parameters. Then for the same case we are going to describe the search for the pseudo-critical behaviour at various quark mass values. We shall discuss the behaviour of the (pseudo-)critical temperature T_c as a function of the (charged) pion mass m_π and the difficulty to extract the chiral limit in order to establish or reject the conjectured $O(4)$-universality. For the two-flavour case we shall further present very recent results for the thermodynamic Equation of State at non-zero temperature. Finally we will provide a view on an ongoing first exploration of QCD thermodynamics under the inclusion of virtual strange and charm quarks at their realistic mass values.

Keywords: Lattice QCD, non-zero temperature, twisted mass fermions, thermodynamic equation of state

1. Introduction

Half a century ago on the basis of a statistical bootstrap model R. Hagedorn has argued that hadrons will have to “boil” at some limiting temperature [1, 2]. Around 15 years later lattice gauge theory simulations provided first numerical evidence for a transition from hadronic matter to a quark-gluon plasma phase [3, 4, 5, 6]. Since that time investigations of the thermodynamics of the quark-gluon system have reached a stage, where its Equation of State (EoS) can be predicted with a reasonable accuracy taking into account up to two quark generations. The EoS providing the pressure p and the energy density ϵ as a function of the temperature T is of large interest as input for the hydrodynamical description of the evolution of the plasma created in relativistic heavy-ion collisions studied at RHIC, BNL and ALICE@LHC, CERN (for a recent introductory review see [7]). At the LHC the quark-gluon plasma (QGP) is produced up to temperatures six times higher than the estimated transition temperature, such that - additionally to the strange quark - the charm quark is expected to give a non-negligible EoS contribution.

On the lattice (for recent reviews see [8, 9, 10, 11, 12]) most efforts were undertaken with $N_f = 2 + 1$ dynamical quark flavour degrees of freedom to reach realistically small values of the u- and d-quark masses, i.e. the physical point, and to reliably extrapolate to the continuum limit [13, 14, 15]. Today the finite-temperature transition from a quark confining and chiral symmetry breaking hadronic phase into a deconfining and chirally symmetric quark-gluon plasma phase at vanishing baryonic chemical potential is known to happen very smoothly at the physical point. Therefore, we often use the notion *crossover* for it.

However, only very few calculations including dynamical charm have been performed until now in the finite-temperature context [16, 17, 18, 19]. These studies - as many others for $N_f = 2+1$ - use computationally cheap improved staggered fermion discretizations at the cost of the theoretical uncertainty of the "rooting trick" applied to the fermionic determinant [20, 21, 22, 23].

Thermodynamics with $N_f = 2$ theoretically safe, but numerically much more expensive Wilson quarks has been extensively studied more than a decade ago by the CP-PACS collaboration [24]. At that time the temperature values $T = 1/(aN_\tau)$ close to the transition temperature T_c were represented by a small number of lattice steps a in the Euclidean time direction ($N_\tau = 4, 6$) and in this way producing strong lattice artifacts. The DIK collaboration continued this effort by enlarging N_τ up to 14 lattice units [25, 26]. More recently improved Wilson fermions were also studied with $N_f = 2 + 1$ dynamical quark flavours on large lattices by the WHOT collaboration [27] and by the Budapest-Wuppertal group [28, 29].

To our knowledge, so far no four-flavour ($N_f = 2 + 1 + 1$) EoS results have been reported using Wilson-type fermionic actions. They would be highly desirable in order to check universality of the outcome of staggered fermion projects.

This article describes the stage achieved with an ongoing lattice QCD project of the tmfT Collaboration, participants of which are (or partly have been) E.-M. Ilgenfritz, K. Jansen, M. Kirchner, M.P. Lombardo, O. Philipsen, C. Pinke, C. Urbach, and L. Zeidlewicz together with the present authors. The project is aimed at studying the high-temperature behaviour near and also beyond the crossover for the Wilson fermion case with a very efficient improvement ansatz in order to handle the approach to the continuum limit. It represents also a special task within a large-scale project of the DFG-funded Transregional Corroborative Research Center *Computational Particle Physics* formulated by K. Jansen and one of the present authors (M.M.-P.). For improvement it employs the Wilson twisted mass discretization of the fermionic action [30, 31, 32] allowing for an automatic $O(a)$ improvement in terms of the lattice spacing a (for a nice review see [33]). Moreover, it relies very much on the simulation methods developed by the European Twisted Mass Collaboration (ETMC) and on its physical zero-temperature results (compare with the contribution by K. Jansen in this edition [34]).

We started with two-flavour QCD and as a first step, we explored the three-dimensional phase diagram spanned in the parameter space of the inverse squared bare coupling β, the bare quark mass m or Wilson hopping parameter κ and of the additionally occuring twisted mass parameter μ. The diagram turned out to be quite complicated [35] with signatures for the strong-coupling Aoki phase [36, 37, 38, 39], the remnant of a first-order bulk transition [40] as well as a cone-shaped surface representing the finite-temperature transition [41].

The next step of our lattice QCD project at $T > 0$ in the presence of $N_f = 2$ dynamical fermion flavour degrees of freedom was the exploration of the finite-temperature crossover phenomenon in the range of pion mass values $m_\pi = 300$ MeV, ..., 500 MeV [42]. The focus was the determination of the (pseudo-) critical temperature T_c from the behaviour of the chiral order parameter, the Polyakov loop and their susceptibilities. Moreover, we checked the universality of the magnetic state equation, and from the dependence of T_c on m_π we tried to extrapolate to the chiral limit in order to confirm or reject $O(4)$ universality of the transition. As a by-product we have computed also the Landau gauge gluon and ghost propagators at non-zero temperature [43] in the context of functional approaches like Dyson-Schwinger equations (see e.g. [44]).

In the following we will report about these earlier steps together with new results on the EoS in the case $N_f = 2$ [45] as well as on first investigations towards the EoS for $N_f = 2 + 1 + 1$ [46]. The central observable of interest is the so-called *trace anomaly* of the energy-momentum tensor or *interaction measure* $I = \epsilon - 3p$ which can be shown to be directly related to the derivative of the average action with respect to the lattice spacing. In both cases for N_f we can rely on the $T = 0$ ETMC results [47, 48, 49, 50, 51, 52, 53] as well as on own simulations in order to fix the lattice spacing in physical units and to carry out necessary subtractions from the $T > 0$ results for I. While for the $N_f = 2$ case the temperature $T = 1/(a(\beta)N_\tau)$ was varied by changing the coupling parameter $\beta = 6/g_0^2$, in the $N_f = 2 + 1 + 1$ case we are applying the fixed-scale approach [27] by varying the number of temporal lattice steps N_τ.

In Section 2 we introduce our lattice discretization setup, while in Section 3 we will discuss the phase diagram of Wilson twisted mass lattice QCD. For the two-flavour case the pseudo-critical behaviour is discussed for several pion mass values in Section 4. For the same case for the first time the evaluation of the EoS is presented in Section 5. First results of the most challenging case of the inclusion of dynamical strange and charm quarks are presented in Section 6. In Section 7 we will draw our conclusions.

2. The Wilson twisted mass setup of lattice QCD

Lattice discretizations of QCD in Euclidean space can be introduced in many different ways. All of them satisfy local gauge invariance but may treat chiral properties as well as improvements with respect to lattice artifacts in a different manner. We decided to follow the choice by ETMC relying on improved versions of the standard Wilson approach [33, 34]. We call them Wilson twisted mass lattice QCD, abbreviated *tmLQCD*.

Thus, we take the following gauge field action

$$\begin{aligned} S_g[U] = \beta \Big(c_0 \sum_P [1 - \frac{1}{3}\mathrm{ReTr}\,(U_P)] \\ + c_1 \sum_R [1 - \frac{1}{3}\mathrm{ReTr}\,(U_R)] \Big), \end{aligned} \tag{1}$$

where U_P and U_R are the parallel transporters around a plaquette loop P and a planar 2×1 rectangular loop R of the gauge field in terms of the lattice link variables $U_{x,\mu} \in SU(3)$. The sums are extended over all plaquettes (P) and all rectangles (R), respectively. As ETMC for the $N_f = 2$ flavour case with the mass-degenerate light quark generation we are employing the tree-level Symanzik improved version ($c_0 = 5/3,\ c_1 = -1/12$), whereas in the extended case of two quark generations including also dynamical strange and charm quarks ($N_f = 2 + 1 + 1$) the Iwasaki version is taken ($c_0 = 3.648,\ c_1 = -0.331$).

The matter field lattice action for the light quark sector reads

$$\begin{aligned} S^l_f[U,\chi_l,\overline{\chi}_l] = \sum_x \overline{\chi}_l(x) \Big(1 - \kappa D_W[U] \\ + 2\mathrm{i}\kappa\mu\gamma_5\tau^3\Big) \chi_l(x), \end{aligned} \tag{2}$$

where the fermion fields are written in the twisted basis $\{\overline{\chi}_l, \chi_l\}$ commonly used for numerical simulations. This basis is related to physical fermion fields $\{\overline{\psi}_l, \psi_l\}$ for *maximal twist* via

$$\psi_l = \frac{1}{\sqrt{2}}(1 + \mathrm{i}\gamma_5\tau^3)\chi_l\,, \quad \overline{\psi}_l = \overline{\chi}_l \frac{1}{\sqrt{2}}(1 + \mathrm{i}\gamma_5\tau^3)\,. \tag{3}$$

The Wilson covariant derivative acts on $\chi(x)$ as

$$\begin{aligned} D_W[U]\chi(x) = \sum_\nu ((1 - \gamma_\nu)\, U_\nu(x)\, \chi(x + \hat{\nu}) \\ + (1 + \gamma_\nu)\, U^\dagger_\nu(x - \hat{\nu})\, \chi(x - \hat{\nu})\Big)\,. \end{aligned} \tag{4}$$

The hopping parameter κ related to the bare (untwisted) quark mass m (in lattice units) via $\kappa \equiv (2m + 8)^{-1}$ has to be set to its coupling dependent critical value $\kappa_c(\beta)$ as determined by ETMC [48] and interpolated to the coupling values used in our studies. The twisted mass parameter μ determines then the degenerate u-, d-quark mass or the (charged) pion mass m_π. The contribution of the strange and charm quark fields to the action in the twisted basis can be represented as

$$\begin{aligned} S^h_f[U,\chi_h,\overline{\chi}_h] = \sum_x \overline{\chi}_h(x)\,[1 - \kappa D_W[U] \\ + 2i\kappa\mu_\sigma\gamma_5\tau^1 + 2\kappa\mu_\delta\tau^3\Big]\chi_h(x)\,, \end{aligned} \tag{5}$$

where the additional twisted mass parameters μ_σ and μ_δ have been introduced. One should keep in mind that the strange and charm quark sectors are intertwined by mixing under renormalization [52] and that parity and flavour breaking effects - in tmLQCD becoming visible mainly by the deviation of the neutral pion mass from the charged pion one - are expected to disappear in the continuum limit.

For studying the non-zero temperature case we simulate the theory with the quantum statistical measure defined by the (Euclidean) partition function

$$\begin{aligned} Z_{QCD} = \int [DU] \int D\overline{\chi}_l D\chi_l D\overline{\chi}_h D\chi_h \times \\ \exp\Big(-S_g[U] - S^l_f[U,\chi_l,\overline{\chi}_l] - S^h_f[U,\chi_h,\overline{\chi}_h]\Big), \end{aligned} \tag{6}$$

where the bosonic gauge field (fermionic quark fields) have necessarily to satisfy periodic (anti-periodic) boundary conditions in the Euclidean time direction x_4 with N_τ lattice steps. The linear three-space extension should satisfy the condition $N_\sigma \gg N_\tau$. In this way we describe a statistical ensemble in a thermodynamic equilibrium at temperature $T = 1/(aN_\tau)$ and in a volume $V = (aN_\sigma)^3$. Z_{QCD} is directly related to the free energy of the system and in principle allows to get other thermodynamic observables as well as to derive the EoS, a matter described later on.

3. Phase diagram of tmLQCD at $T > 0$

The β-κ phase diagram for two-flavour lattice QCD with clover-improved Wilson fermions has been thoroughly studied for small time-extent $N_\tau = 4, 6$ almost 15 years ago by the CP-PACS collaboration [54, 24]. A schematic view of the emerging phase structure is shown in Fig. 1. The cusp of the strong coupling Aoki phase [36, 37, 38, 39, 55] – the latter (in the infinite-volume limit) characterized by a non-vanishing expectation value $\langle\overline{\psi}\mathrm{i}\gamma_5\tau^3\psi\rangle$ indicating the spontaneous breakdown of a combined parity-flavour symmetry – seemed tightly connected with the thermal transition line $\kappa_t(\beta)$.

Here, we consider again $N_f = 2$ Wilson fermions but with the additional twisted mass term $\mu\,\overline{\chi}\mathrm{i}\gamma_5\tau^3\chi$. Having included this term a more complicated 3D phase diagram emerges as long as κ is not yet fixed to its critical value κ_c corresponding to vanishing m_π. We have investigated this phase diagram by computing various "observables" like plaquette and Polyakov loop expectation values and susceptibilities, the corresponding autocorrelation times as well as the so-called pion norm along several trajectories (compare with [56, 35]).

For a lattice size with $N_\tau = 8, N_\sigma = 16$, we were able to show [35] that the Aoki phase ends somewhere inside the interval $\beta = 3.0, \ldots, 3.4$. Around $\beta = 3.4$, it becomes replaced by a region of metastabilities indicating a first order transition area (the shaded area in Fig. 2), a remnant of a transition known also in the zero-temperature case [57, 58, 40, 59].

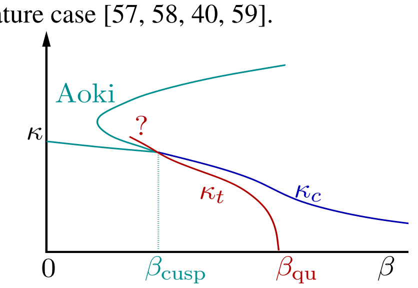

Figure 1: Schematic view of the phase structure as seen in older investigations [24] for a temporal lattice extent $N_\tau = 4, 6$.

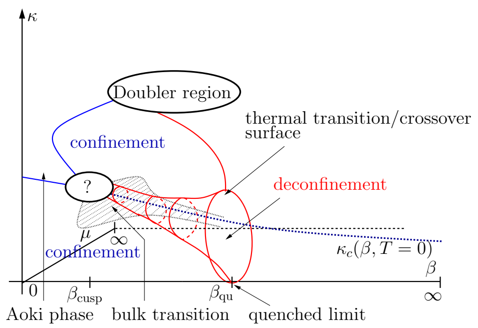

Figure 2: Schematic view of the phase structure as found in our work [35] with twisted mass fermions in the β-κ-μ diagram for $N_\tau = 8$.

In what follows we are concentrating on the thermal transition seen at not too small μ (otherwise we are still running into the metastability region). Since the hopping parameter κ and the twisted mass parameter μ are directly connected with the bare quark mass

$$m_q = \sqrt{\frac{1}{4}\left(\frac{1}{\kappa} - \frac{1}{\kappa_c}\right)^2 + \mu^2}\,, \tag{7}$$

we wanted to see the cone-like structure of surfaces of equal physics around the critical chiral line $\kappa = \kappa_c(\beta)$, $\mu = 0$. For this aim we scanned the phase diagram in a larger κ-range in order to see how the thermal transition surface extends above $\kappa_c(\beta)$. The result is shown in the left panel of Fig. 3. For values $\beta = 3.4, 3.45, 3.65, 3.75$ from the steep rise of the Polyakov loop

$$\mathrm{Re}\left(\langle L\rangle\right) = \frac{1}{N_\sigma^3}\mathrm{Re}\langle\frac{1}{N_c}\mathrm{Tr}\sum_{\mathbf{x}}\prod_{x_4=1}^{N_\tau} U_4\left(\mathbf{x}, x_4\right)\rangle \tag{8}$$

(and also from maxima of its susceptibility not shown here) we observe very clear signals for a thermal transition in κ. But additionally, for $(\beta = 3.75, \mu = 0.005)$, we see a tiny κ-interval around $\kappa_c = 0.166$ where the Polyakov loop exhibits a comparably small maximum, which could have been easily overlooked. The latter maximum becomes better visible by zooming into the region around $\kappa_c(\beta)$ also at larger β-values, see the right panel of Fig. 3. For the Polyakov loop susceptibility (not shown here) with rising β we found already two clear maxima at $\beta = 3.8$, $\kappa \simeq 0.1635, 0.1660$, i.e. not far from $\kappa_c \simeq 0.1640$ [35].

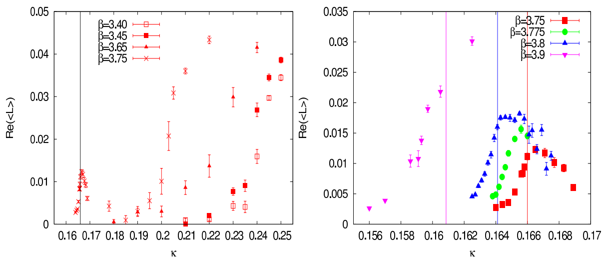

Figure 3: **Left**: κ-scans of the Polyakov loop for various β-values ($\beta = 3.4, 3.45, 3.65$ for $\mu = 0.0068$; $\beta = 3.75$ for $\mu = 0.005$). Vertical lines mark $\kappa_c(\beta = 3.75)$. **Right**: Real part of the Polyakov loop for $\beta = 3.75, 3.775, 3.8, 3.9$ and $\mu = 0.005$. Vertical lines mark $\kappa_c(\beta)$ for $\beta = 3.9, 3.8, 3.75$ from left to right. See also [35].

Thus, with rising κ starting from values below κ_c we pass through subsequent confinement-deconfinement, deconfinement-confinement transitions (or better crossovers) below and above κ_c, respectively, followed again by a confinement-deconfinement transition far above κ_c. The latter transition surface extends to the next fermion doubler region in the phase diagram. We have seen by additional β-scans at fixed $\kappa > \kappa_c(\beta)$ that the Creutz cone structure [41] that we are exploring is connected with the upper confinement-deconfinement transition by a phase transition surface bending upward in κ at larger β. We tried to figure out also how far the crossover or transition cone extends in the μ-direction. From κ-scans for the Polyakov loop at $\beta = 3.75$ and various μ-values we could conclude that the inner region of the cone there is restricted to the interval $0.014 < \mu < 0.025$.

Note that at $\beta = 3.75$ and $\kappa_c(\beta) = 0.166$ the value $\mu = 0.005$ can be related to a pion mass value $m_\pi \simeq$

400 MeV and a temperature $T \simeq 210$ MeV, i.e. values to which we come back later.

Finally, in a recent master thesis [60] for small $N_\tau = 4$ and at maximal twist $\kappa_c(\beta)$ it was shown that for large enough β one finds signatures for a first order critical line $\mu = \mu_t(\beta)$ very similar to the line $\kappa = \kappa_t(\beta)$ in the κ-β plane close to the first order transition in pure $SU(3)$ gauge theory.

Having understood the cone shape of the finite-temperature transition or crossover in the β-κ-μ phase diagram, we have always fixed κ at its maximal twist value in order to ensure $O(a)$ improvement.

4. Pseudocritical behaviour for $N_f = 2$

At present for studies of the crossover behaviour we are relying on simulations at (charged) pion masses $m_\pi \simeq \{290, 360, 430 \text{ and } 640\}$ MeV (for historical reasons we call these ensembles A, B, C, and D). Compared to our previous paper [42] we have extended the analysis for the ensembles B and C from lattice sizes $12 * 32^3$ and $12 * 24^3$ to ones with smaller N_τ. The ensemble D with a lattice size $10 * 24^3$ is new [45]. The scale setting via the Sommer scale parameter r_0 [61] has been repeated on larger sets of simulations at $T = 0$ with elongated lattices in the meantime, which has slightly shifted our values for m_π and also the estimates of the pseudo-critical temperatures. The latter are determined from the variance of $\overline{\psi}\psi$ over the gauge ensembles

$$\sigma^2_{\overline{\psi}\psi} = \frac{V}{T}\left(\left\langle(\overline{\psi}\psi)^2\right\rangle - \left\langle\overline{\psi}\psi\right\rangle^2\right). \tag{9}$$

It corresponds to the disconnected part of the usual chiral susceptibility and should show a maximum in the region of T_c [62]. This is indeed the case for all our ensembles. The two representative cases B,D are shown in the two upper panels of Fig. 4. From fitting a Gaussian function to the $N_\tau = 12$ data of $\sigma^2_{\overline{\psi}\psi}$ around the maxima we extract the values of the pseudo-critical couplings β_c that are converted to a physical value of T_c using an interpolation of $a(\beta)$ [42, 45]. At leading order in chiral perturbation theory and for a phase transition of second order the pion mass dependence of T_c is expected to be given as [63, 64]

$$T_c(m_\pi) = T_c(0) + A\, m_\pi^{2/(\tilde{\beta}\delta)}, \tag{10}$$

where $T_c(0)$ is the critical temperature in the chiral limit and $\tilde{\beta}$ and δ are critical exponents corresponding to the universality class of second order phase transitions. We have restricted ourselves to the chiral scenarios discussed in [42] including a first order scenario as well as the $O(4)$ and $Z(2)$ second order scenarios, for the latter assuming a second order endpoint located at $m_{\pi,c} = 0$ MeV or alternatively at $m_{\pi,c} = 200$ MeV. The result of fits of Eq. (10) to our data is shown in the lower panel of Fig. 4. As the fitted curves are all describing the given data quite well we conclude that the present set of pion mass values can not discriminate among the different chiral scenarios that have been studied. For the $O(4)$ model the fit prefers a value of $T_c(0) = 150$ (26) MeV.

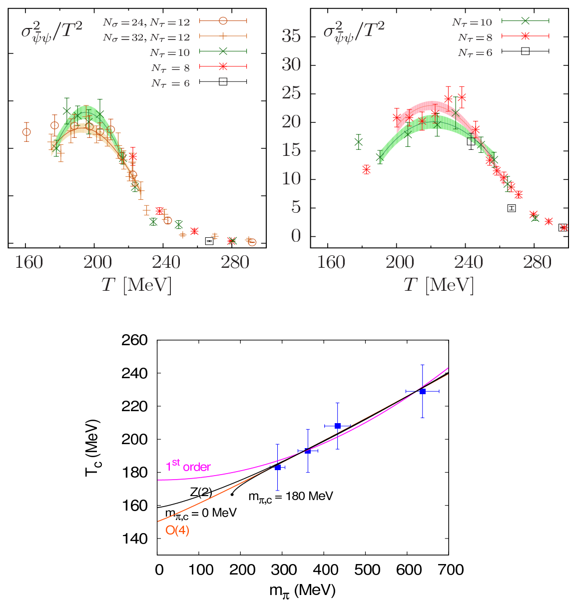

Figure 4: Upper panels: Determination of T_c from $\sigma^2_{\overline{\psi}\psi}$ using a Gaussian fit to the maxima for the B (left) and D (right) ensembles with various lattice sizes (see [45]). Lower panel: T_c versus m_π determined from the ensembles A12, B12, C12, D10 together with fits representing different scenarios for the chiral limit. The notation A12, ... indicates the linear lattice size in the x_4-direction $N_\tau = 12, \ldots$ (compare with [42]).

Here we have not shown the other main observable of our investigations, the Polyakov loop and its susceptibility. The Polyakov loop as a function of the temperature represents an order parameter for the deconfinement transition in the limit of infinitely heavy quarks. It can be used to locate the crossover region also at varying quark mass from its inflexion point T_{inf} along its rise with T. Taking into account a proper renormalization of the Polyakov loop for the different ensembles at given m_π-values we found T_{inf} always above T_c [42, 45].

5. Equation of state for $N_f = 2$

For deriving the EoS we start from the trace anomaly of the energy-momentum tensor $I(T) = \Theta^{\nu\nu}$ related to the partition function by a total derivative with respect to the lattice spacing a along lines of constant physics (LCP):

$$\frac{I}{T^4} = \frac{\epsilon - 3p}{T^4} = -\frac{1}{T^3 V}\left(\frac{d\ln Z}{d\ln a}\right)_{\rm sub} = T\frac{\partial}{\partial T}\left(\frac{p(T)}{T^4}\right). \tag{11}$$

It is related to the pressure p (and to the energy density ϵ) via integrating the last relation [65]. $(\ldots)_{\rm sub}$ means that all expectation values are rendered finite by subtracting the corresponding vacuum expectation values at $T = 0$. The trace anomaly I contains derivatives of the expectation values of all the terms in the lattice action $S = \sum_i b_i S_i$ with respect to the bare coupling and mass parameters b_i and those of b_i to the lattice spacing a:

$$\begin{aligned}\frac{I}{T^4} &= \frac{1}{T^3 V}\sum_i a\frac{db_i}{da}\left\langle\frac{\partial S}{\partial b_i}\right\rangle_{\rm sub} \\ &= N_\tau^4 B_\beta \frac{1}{N_\sigma^3 N_\tau}\left\{\frac{c_0}{3}\left\langle {\rm ReTr}\sum_P U_P\right\rangle_{\rm sub}\right. \\ &\quad +\frac{c_1}{3}\left\langle {\rm ReTr}\sum_R U_R\right\rangle_{\rm sub} \\ &\quad +B_\kappa \langle\bar\chi_l D_{\rm W}[U]\chi_l\rangle_{\rm sub} \\ &\quad \left. -\left[2(a\mu)B_\kappa + 2\kappa_c(a\mu)B_\mu\right]\left\langle\bar\chi_l i\gamma_5\tau^3\chi_l\right\rangle_{\rm sub}\right\},\end{aligned} \tag{12}$$

where the coefficients B_i are

$$B_\beta = -a\frac{d\beta}{da}, \quad B_\mu = \frac{1}{(a\mu)}\frac{\partial(a\mu)}{\partial\beta}, \quad B_\kappa = \frac{\partial\kappa_c}{\partial\beta}. \tag{13}$$

Later on, in the four-flavour case $N_f = 2+1+1$, one has to add the terms related to the heavy fermion action according to Eq. (5). We shall subtract terms in I/T^4 which by employing a Symanzik expansion turn out to be lattice artifacts of order $O(a^2)$ in the limit of maximal twist. For a derivation of this observation as well as for a discussion of the $T = 0$ subtractions and of the evaluation of the B-functions we refer to [45, 66]. How well we were able to stay on the LCP while varying β, $\kappa = \kappa_c(\beta)$, and $\mu(\beta)$ can be judged from our plot of the pion mass versus β (or temperature T) in Fig. 5.

In Fig. 6 we show our final result for the trace anomaly for the ensembles B, D of the pseudoscalar masses under investigation [45]. In all cases we have observed sizeable lattice artifacts in the height of the maximum and even in the falling edge at larger temperatures. This is the reason, why we have employed a tree-level correction as described in [13] which corrects the trace anomaly by the continuum-to-lattice ratio of the Stefan-Boltzmann limit values for the pressure (see Ref. [67] for the Symanzik-improved gauge action and [68] for the twisted mass fermion action). For a temperature value close to the peak position of the trace anomaly and at some higher temperature we have checked the continuum limit extrapolations with and without tree-level corrections. For $a \to 0$ the values were found to approach each other within the estimated errors. For the corrected case - as expected - the a-dependence turned out to be clearly weaker.

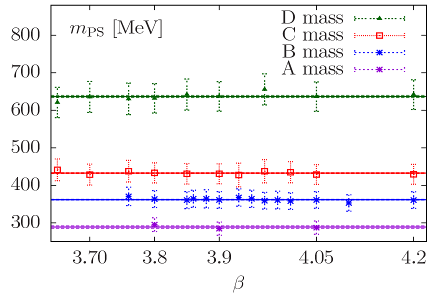

Figure 5: Pion mass values versus β as a quality check for our lines of constant physics for all four fermion mass ensembles considered.

The peak value of the trace anomaly is a good indicator for the universality of the results of different approaches. We notice that our peak value $\simeq 3$ for $N_f = 2$ only weakly depends on the mass and lies in between the values for the pure gauge case ($N_f = 0$) [69] and the one for $N_f = 2+1$ at the physical point [15].

The evaluation of the pressure from the integral technique proceeds by integrating the identity $\frac{I}{T^4} = T\frac{\partial}{\partial T}\left(\frac{p}{T^4}\right)$ with respect to the temperature along a LCP

$$\frac{p}{T^4} - \frac{p_0}{T_0^4} = \int_{T_0}^{T} d\tau \left.\frac{\epsilon - 3p}{\tau^5}\right|_{\rm LCP}. \tag{14}$$

We perform the integration Eq. (14) after having fitted the following ansatz [13] to the available lattice data

$$\begin{aligned}\frac{I}{T^4} &= \left(1 + \frac{a_2}{N_\tau^2}\right)\cdot\exp\left(-h_1\bar t - h_2\bar t^2\right) \\ &\quad\times\left(h_0 + \frac{f_0\{\tanh(f_1\bar t + f_2)\}}{1 + g_1\bar t + g_2\bar t^2}\right),\end{aligned} \tag{15}$$

where $\bar t = T/T_0$ and T_0 is a free parameter in the fit.

Our final results for the pressure and the energy density as functions of the temperature are shown in Fig. 7 for the ensembles B and D, respectively [45].

6. Towards thermodynamics with $N_f = 2+1+1$

As a next step we have started to investigate the QCD thermodynamics taking into account strange and charm quark degrees of freedom at their realistic mass values

$m_\pi^\pm$ [MeV]	a [fm]	$N_\tau \times N_\sigma^3$	statistics
364	0.0936	$\{5,6,7,8,9,10,11,12\} \times 24^3$	2k-7k
		$\{13,14\} \times 32^3$	5k,27k
372	0.0823	$\{6,7,8,10,11,12,13,14,15,16\} \times 32^3$	2k-27k

Table 1: $N_f = 2+1+1$ gauge field ensembles data of which are presented here. Lattice spacings are adopted from Ref. [70].

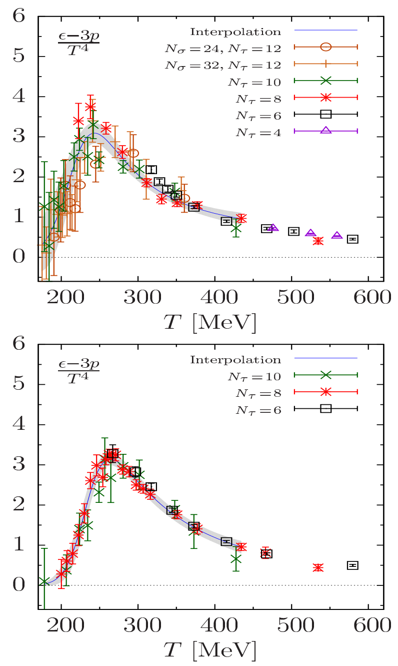

Figure 6: The tree-level corrected trace anomaly for the $N_f = 2$ B mass (upper panel) and D mass (lower panel) ensembles obtained for different values of the temporal extent N_τ. Also shown is the result of combined fits of the interpolation formula Eq. (15) to the $N_\tau = 8, 10$ and 12 data (the latter only for the B case). For the B mass the results obtained on the smaller spatial volume ($N_\sigma = 24$) are superimposed slightly shifted for better visibility. The latter data however has not been included in the fit (see [45]).

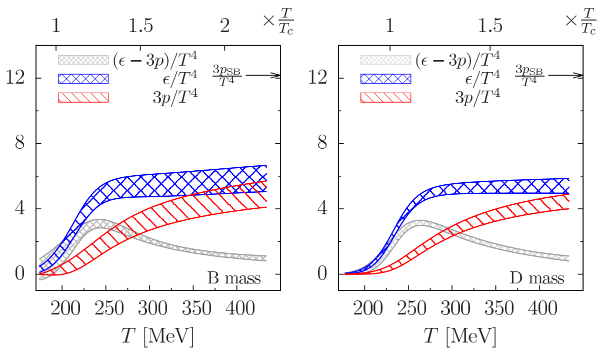

Figure 7: Final result for pressure p and the energy density ϵ in units of T^4 for the $N_f = 2$ B (left) and D (right) mass ensembles [45]. The interpolation of the trace anomaly used for integrating the pressure is also shown. The arrow indicates the expected Stefan-Boltzmann limit for the pressure. On top of the figures we indicate the temperature in units of T_c.

(see Eq. (5)) in a large interval of temperatures. The charm degrees of freedom are expected to become visible in the EoS at sufficiently high temperatures above T_c.

In order to fix the scale and to determine the scale-dependent coefficients in the trace anomaly on the basis of already existing ETMC-data we decided to employ the fixed-scale approach in varying the temperature $T = 1/(N_\tau a)$ by changing N_τ [27]. In this way we are in the position to consider pion mass cases of approximately 370 MeV at different lattice spacings [70] (see Table 1), nicely allowing us to compare with the $N_f = 2$ case, where we studied a 360 MeV pion mass (B ensembles).

We have computed the renormalized Polyakov loop and also an appropriately subtracted light fermion chiral condensate ratio defined in [42] as a function of the temperature. Having done for $N_f = 2$ a new scale fixing with more ensembles and better statistics [45] we see the curves with similar pion masses of 360 − 370 MeV to be slightly shifted towards lower temperature values for $N_f = 2+1+1$ as compared to $N_f = 2$ (see also our preliminary presentation in [46]). Taking the strange quark into account one can eliminate the divergence in the light quark condensate by suitably subtracting the strange quark condensate [71]:

$$\Delta_{l,s} = \frac{\langle\overline{\psi}\psi\rangle_l - \frac{\mu}{\mu_s}\langle\overline{\psi}\psi\rangle_s}{\langle\overline{\psi}\psi\rangle_l^{T=0} - \frac{\mu}{\mu_s}\langle\overline{\psi}\psi\rangle_s^{T=0}}\,, \qquad (16)$$

where μ and μ_s denote the bare light and strange quark masses. The strange quark condensate has been obtained in the Osterwalder-Seiler setup [72, 31] which avoids mixing in the heavy quark sector. The mass μ_s has been determined as to reproduce the physical $\bar{s}\gamma_\mu s$-mass. The quantity $\Delta_{l,s}$ does not show visible lattice spacing artefacts over the whole range of temperatures and exhibits a smooth order parameter behaviour (see the left panel of Fig. 8).

The unrenormalized disconnected part of the chiral susceptibility according to Eq. (9) can be nicely compared with that of the B ensemble in the $N_f = 2$ case with a similar pseudoscalar mass. The pseudo-critical

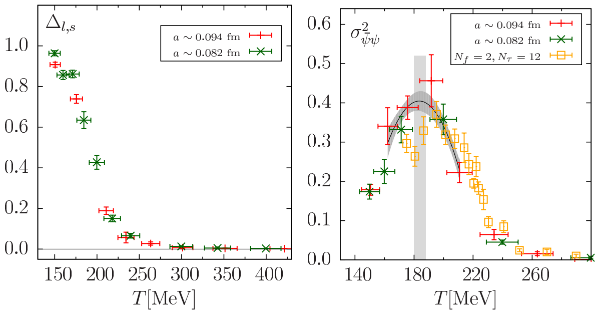

Figure 8: **Left**: Subtracted (renormalized) chiral condensate vs. T at $m_\pi \simeq 370$ MeV for $N_f = 2+1+1$. **Right**: Light quark chiral susceptibility vs. T at $m_\pi \simeq 370$ MeV for $N_f = 2+1+1$ and for the $N_f = 2$ B12 ensemble with $m_\pi \simeq 360$ MeV.

	$N_f = 2+1+1$	$N_f = 2$
T_c [MeV]	184(4)	193(13)

Table 2: Pseudo-critical temperatures obtained from chiral susceptibilities at $m_\pi \simeq 370$ MeV ($N_f = 2+1+1$) and $m_\pi \simeq 360$ MeV ($N_f = 2$), respectively.

T_c value at $N_f = 2+1+1$ is somewhat smaller (see the right panel of Fig. 8). From a Gaussian fit we obtain values as shown in Table 2.

7. Conclusions

In this report we gave a short overview of investigations of the QCD thermodynamics within the lattice approach employing dynamical Wilson fermions with twisted mass terms in order to ensure automatic $O(a)$ improvement as advocated by the ETM Collaboration. Our computations were carried out by a joint effort of the tmfT Collaboration. As one normally has to do, we started with an exploration of the phase diagram of the lattice theory in the three-dimensional β-κ-μ space. The phase structure turned out to be rather complicated but locates the finite-temperature transition or crossover on a cone-shape (pseudo-)critical surface.

Tuning our bare κ to its critical, i.e. maximal twist value of vanishing pion mass we were then able to investigate the crossover behaviour in the two-flavour case at several pion mass values ranging from 290 MeV to 640 MeV. Measuring the Polyakov loop, the chiral condensate and the disconnected part of the chiral susceptibility allowed us to locate the crossover region and to show the dependence of the chiral (pseudo-) critical temperature T_c as a function of the (charged) pion mass m_π. Unfortunately, the m_π values turned out to be still too large in order to discriminate between different scenarios of approaching criticality in the chiral limit and therefore to decide the fundamental question, whether the transition in this limit is of first or second order. In the same two-flavour case we have shown also results of a careful pilot computation of the EoS in the Wilson twisted mass setup. For this aim the trace anomaly or interaction measure was computed as a function of the temperature. A tree-level correction of the results allowed nicely to approach the continuum limit with lattices of $N_\tau = 12$ Euclidean time steps.

Finally, we have presented first results of a fixed scale finite-temperature study of the QCD crossover with a full dynamical second quark generation. We have concentrated on a single pion mass value at several lattice spacings in order to estimate cutoff effects. From the maximum of the disconnected part of the bare chiral susceptibility we have estimated the temperature of the chiral crossover and found it slightly shifted compared with the $N_f = 2$ case.

We are currently working on the analysis of the EoS with the inclusion of the dynamical strange and charm contributions at the same pion mass value as well as on the data analysis at a pion mass well below 300 MeV.

Acknowledgments

The authors express their deep gratitude to their tmfT collaborators for fruitful joint work. They acknowledge the generous support by the DFG-funded Corroborative Research Center SFB/TR 9 and also by the ETM Collaboration, in particular by Karl Jansen. We are grateful to the HLRN supercomputing centers Berlin and Hannover. For generating gauge configurations and statistical analysis we have used the open source packages tmLQCD[73, 74] and R[75], respectively.

References

[1] R. Hagedorn, Nuovo Cim.Suppl. 3 (1965) 147.
[2] R. Hagedorn, Nuovo Cim. A56 (1968) 1027.
[3] L. Susskind, Phys.Rev. D20 (1979) 2610.
[4] L. D. McLerran, B. Svetitsky, Phys.Lett. B98 (1981) 195.
[5] J. Kuti, J. Polonyi, K. Szlachanyi, Phys.Lett. B98 (1981) 199.
[6] J. Engels, F. Karsch, H. Satz, I. Montvay, Phys.Lett. B101 (1981) 89.
[7] W. Florkowski, `arXiv:1410.7904`.
[8] C. DeTar, `arXiv:1101.0208`.
[9] L. Levkova, PoS LATTICE2011 (2011) 011. `arXiv:1201.1516`.
[10] O. Philipsen, Prog.Part.Nucl.Phys. 70 (2013) 55. `arXiv:1207.5999`.
[11] P. Petreczky, J.Phys. G39 (2012) 093002. `arXiv:1203.5320`.
[12] M. P. Lombardo, PoS (LATTICE 2012) (2012) 016. `arXiv:1301.7324`.
[13] S. Borsanyi, G. Endrodi, Z. Fodor, A. Jakovac, S. D. Katz, S. Krieg, C. Ratti, K. K. Szabo, JHEP 1011 (2010) 077. `arXiv:1007.2580`.
[14] S. Borsanyi, Z. Fodor, C. Hoelbling, S. D. Katz, S. Krieg, K. K. Szabo, Phys.Lett. B730 (2014) 99. `arXiv:1309.5258`.

[15] A. Bazavov, et al., Phys.Rev. D90 (2014) 094503. arXiv:1407.6387.
[16] A. Bazavov, et al., PoS LATTICE2012 (2012) 071.
[17] A. Bazavov, et al., PoS LATTICE2013 (2014) 154. arXiv:1312.5011.
[18] C. Ratti, S. Borsanyi, G. Endrodi, Z. Fodor, S. D. Katz, et al., Nucl.Phys. A904-905 (2013) 869c.
[19] S. Borsanyi, Z. Fodor, C. Hoelbling, S. D. Katz, S. Krieg, et al., arXiv:1410.7917.
[20] B. Bunk, M. Della Morte, K. Jansen, F. Knechtli, Nucl.Phys. B697 (2004) 343. arXiv:hep-lat/0403022.
[21] M. Creutz, Phys.Lett. B649 (2007) 230. arXiv:hep-lat/0701018.
[22] C. Bernard, M. Golterman, Y. Shamir, S. R. Sharpe, Phys.Rev. D78 (2008) 078502. arXiv:0808.2056.
[23] M. Creutz, PoS (Confinement8) (2008) 016. arXiv:0810.4526.
[24] A. Ali Khan, et al., Phys.Rev. D64 (2001) 074510. arXiv:hep-lat/0103028.
[25] V. Bornyakov, R. Horsley, S. Morozov, Y. Nakamura, M. Polikarpov, P. Rakow, G. Schierholz, Phys. Rev. D82 (2010) 014504. arXiv:0910.2392.
[26] V. Bornyakov, R. Horsley, Y. Nakamura, M. Polikarpov, P. Rakow, et al., PoS Lattice2010 (2014) 170. arXiv:1102.4461.
[27] T. Umeda, S. Aoki, S. Ejiri, T. Hatsuda, K. Kanaya, H. Ohno, Y. Maezawa, Phys.Rev. D85 (2012) 094508. arXiv:1202.4719.
[28] S. Borsanyi, Z. Fodor, C. Hoelbling, S. D. Katz, S. Krieg, et al., PoS LATTICE2011 (2011) 209. arXiv:1111.3500.
[29] S. Borsanyi, S. Dürr, Z. Fodor, C. Hoelbling, S. D. Katz, et al., JHEP 1208 (2012) 126. arXiv:1205.0440.
[30] R. Frezzotti, G. C. Rossi, JHEP 08 (2004) 007. arXiv:hep-lat/0306014.
[31] R. Frezzotti, G. Rossi, JHEP 0410 (2004) 070. arXiv:hep-lat/0407002.
[32] R. Frezzotti, et al., JHEP 04 (2006) 038. arXiv:hep-lat/0503034.
[33] A. Shindler, Phys. Rept. 461 (2008) 37. arXiv:0707.4093.
[34] K. Jansen, Simulations with exact and chirally improved fermions, Advances in Computational Particle Physics, this volume (2014).
[35] E.-M. Ilgenfritz, K. Jansen, M. Lombardo, M. Müller-Preussker, M. Petschlies, O. Philipsen, L. Zeidlewicz, Phys. Rev. D80 (2009) 094502. arXiv:0905.3112.
[36] S. Aoki, Phys.Rev. D30 (1984) 2653. doi:10.1103/PhysRevD.30.2653.
[37] S. Aoki, A. Gocksch, Phys.Rev. D45 (1992) 3845.
[38] S. R. Sharpe, J. Singleton, R. L., Phys.Rev. D58 (1998) 074501. arXiv:hep-lat/9804028.
[39] E.-M. Ilgenfritz, W. Kerler, M. Müller-Preussker, A. Sternbeck, H. Stüben, Phys.Rev. D69 (2004) 074511. arXiv:hep-lat/0309057.
[40] G. Münster, JHEP 0409 (2004) 035. arXiv:hep-lat/0407006.
[41] M. Creutz, Phys.Rev. D76 (2007) 054501. arXiv:0706.1207.
[42] F. Burger, E.-M. Ilgenfritz, M. Kirchner, M. Lombardo, M. Müller-Preussker, O. Philipsen, C. Urbach, L. Zeidlewicz, Phys.Rev. D87 (2013) 074508. arXiv:1102.4530.
[43] R. Aouane, F. Burger, E.-M. Ilgenfritz, M. Müller-Preussker, A. Sternbeck, Phys.Rev. D87 (2013) 114502. arXiv:1212.1102.
[44] C. S. Fischer, J. Luecker, C. A. Welzbacher, Phys.Rev. D90 (2014) 034022. arXiv:1405.4762.
[45] F. Burger, E.-M. Ilgenfritz, M. P. Lombardo, M. Müller-Preussker, arXiv:1412.6748.
[46] F. Burger, G. Hotzel, M. Müller-Preussker, E.-M. Ilgenfritz, M. P. Lombardo, PoS (LATTICE 2013) (2013) 153. arXiv:1311.1631.
[47] P. Boucaud, et al., Phys.Lett. B650 (2007) 304. arXiv:hep-lat/0701012.
[48] P. Boucaud, et al., Comput.Phys.Commun. 179 (2008) 695. arXiv:0803.0224.
[49] R. Baron, et al., JHEP 1008 (2010) 097. arXiv:0911.5061.
[50] R. Baron, et al., PoS LAT2009 (2009) 104. arXiv:0911.5244.
[51] R. Baron, et al., JHEP 1006 (2010) 111. arXiv:1004.5284,
[52] R. Baron, et al., Comput.Phys.Commun. 182 (2011) 299. arXiv:1005.2042.
[53] R. Baron, et al., PoS (LATTICE 2010) (2010) 123. arXiv:1101.0518.
[54] A. Ali Khan, et al., Phys. Rev. D63 (2001) 034502. arXiv:hep-lat/0008011.
[55] E.-M. Ilgenfritz, W. Kerler, M. Müller-Preussker, A. Sternbeck, H. Stüben, arXiv:hep-lat/0511059.
[56] M. Müller-Preussker, et al., PoS (Lat2009) (2009) 266. arXiv:0912.0919.
[57] S. R. Sharpe, J. M. Wu, Phys.Rev. D70 (2004) 094029. arXiv:hep-lat/0407025.
[58] F. Farchioni, R. Frezzotti, K. Jansen, I. Montvay, G. Rossi, et al., Eur.Phys.J. C39 (2005) 421. arXiv:hep-lat/0406039.
[59] F. Farchioni, K. Jansen, I. Montvay, E. Scholz, L. Scorzato, et al., Eur.Phys.J. C42 (2005) 73. arXiv:hep-lat/0410031.
[60] W. Tomberg, Master Thesis, Humboldt University Berlin (2014) 1–91.
[61] R. Sommer, Nucl.Phys. B411 (1994) 839. arXiv:hep-lat/9310022.
[62] C. W. Bernard, T. Blum, C. E. Detar, S. A. Gottlieb, U. M. Heller, et al., Phys.Rev.Lett. 78 (1997) 598. arXiv:hep-lat/9611031.
[63] F. Karsch, Phys. Rev. D49 (7) (1994) 3791. doi:10.1103/PhysRevD.49.3791.
[64] Y. Iwasaki, et al., Phys. Rev. Lett. 78 (1997) 179. arXiv:hep-lat/9609022.
[65] C. DeTar, U. Heller, Eur.Phys.J. A41 (2009) 405. arXiv:0905.2949.
[66] F. Burger, G. Hotzel, K. Jansen, M. Petschlies, arXiv:1412.0546.
[67] F. Karsch, E. Laermann, A. Peikert, Phys.Lett. B478 (2000) 447. arXiv:hep-lat/0002003.
[68] O. Philipsen, L. Zeidlewicz, Phys. Rev. D81 (2010) 077501. arXiv:0812.1177.
[69] S. Borsanyi, G. Endrodi, Z. Fodor, S. Katz, K. Szabo, JHEP 1207 (2012) 056. arXiv:1204.6184.
[70] C. Alexandrou, V. Drach, K. Jansen, C. Kallidonis, G. Koutsou, Phys.Rev. D90 (2014) 074501. arXiv:1406.4310.
[71] M. Cheng, N. Christ, S. Datta, J. van der Heide, C. Jung, et al., Phys.Rev. D77 (2008) 014511. arXiv:0710.0354.
[72] K. Osterwalder, E. Seiler, Annals Phys. 110 (1978) 440.
[73] K. Jansen, C. Urbach, Comput.Phys.Commun. 180 (2009) 2717–2738. arXiv:0905.3331.
[74] A. Abdel-Rehim, F. Burger, A. Deuzeman, K. Jansen, B. Kostrzewa, L. Scorzato, C. Urbach, PoS LATTICE2013 (2014) 414. arXiv:1311.5495.
[75] R Development Core Team, R: A language and environment for statistical computing, Vienna, Austria (2010). URL http://www.R-project.org.